

# Integrated back and forward analysis of rock slope stability and rockslide runout at Afternoon Creek, Washington

Alex Strouth and Erik Eberhardt

**Abstract:** Hazard assessments involving large rock slopes are often problematic, given the influence of geology on failure kinematics and the subsequent influence of the failure kinematics on the rockslide runout. The 2003 Afternoon Creek rockslide in northwest Washington is one such example, where 750 000 m<sup>3</sup> of rock slid from a steep ridge harmlessly into Afternoon Creek. However, topographic and structural controls at the source area unexpectedly redirected a small volume (<10%) down the opposite side of the ridge along a much steeper travel path, impacting the highway below. Postfailure investigations indicate that the slope still presents a danger. To address this, a framework was developed that links back analyses with forward modelling of failure initiation and runout. Field mapping and data collection were specifically tailored for these analyses. Advanced numerical modelling was used to assess likely rockslide source areas, volumes, and controlling features. These were then used to guide a series of three-dimensional runout simulations to model rockslide travel path, reach, and velocities. The results show that a rockslide originating from the ridge could occur again and that the topography would again direct a small percentage of material down the backside which would reach the highway below.

*Key words:* rockslide, hazard assessment, LiDAR, distinct-element modelling, runout analysis.

**Résumé :** L'évaluation des dangers impliquant des grandes pentes rocheuses sont souvent problématiques puisqu'il faut tenir compte de l'influence de la géologie sur la cinématique des ruptures, et de l'influence subséquente de la cinématique des ruptures sur le parcours du glissement rocheux. Le glissement rocheux de 2003 de Afternoon Creek, dans le nord-ouest de Washington, en est un exemple, où 750, 000 m<sup>3</sup> de roche ont glissé d'une pente raide jusque dans Afternoon Creek sans causer de dommages. Cependant, des éléments topographiques et structuraux à la source du glissement ont redirigé de façon inattendue un petit volume (< 10 %) de l'autre côté de la crête et dans un parcours plus abrupt; ces roches ont fini par impacter l'autoroute située au bas. Des investigations post-rupture ont indiqué que la pente présente encore un danger. Un plan de travail a été élaboré pour évaluer la situation, qui relie des rétro-analyses et des modélisations en amont de l'initiation de la rupture et du parcours. La cartographie du terrain et la collecte de données se sont faites spécifiquement pour ces analyses. De la modélisation numérique avancée a été utilisée pour déterminer les sources probables de glissements rocheux, leurs volumes et les caractéristiques qui les contrôlent. Ces informations ont servi ensuite à guider une série de simulations 3D de parcours pour modéliser la trajectoire, l'étendue et la vitesse d'un glissement rocheux. Les résultats montrent qu'un glissement provenant de la crête peut se produire encore, et que la topographie redirigerait une fois de plus un petit pourcentage du matériel vers l'arrière de la crête, ce qui atteindrait l'autoroute au bas de la pente.

*Mots-clés :* glissement rocheux, évaluation du danger, LiDAR, modélisation par éléments distincts, analyse de parcours.

[Traduit par la Rédaction]

## Introduction

A methodology that combines several numerical techniques, linking rockslide initiation to runout, was used to investigate an unstable rock slope at Afternoon Creek in northwest Washington, USA (Fig. 1). The hazard characterization study was carried out in response to a rock slope failure that occurred at the site in November 2003, involving

approximately 750 000 m<sup>3</sup> of jointed orthogneiss rock. Most of the slide mass travelled into and down a sloping creek bed (Afternoon Creek; Fig. 1), coming to rest on older deposits of rockslide and rockfall material. However, a small portion (<10%) displaced in a different direction from that of the main mass because of complex topographic and structural geology controls at the source area and travelled down a steeper path on the opposite side of the ridge, impacting and destroying a section of state highway (Washington State Route 20 or SR-20).

The potential for future rock slope failures at this site poses a challenge to the selection and design of appropriate hazard mitigation schemes, given the uncertainty in slide kinematics and its controlling influence on runout path. To address this issue, a detailed hazard characterization study was carried out to study the mechanism of the November 2003 rockslide; characterize the postfailure motion of the debris; and estimate the location, volume, and runout paths

Received 12 November 2008. Accepted 9 April 2009. Published on the NRC Research Press Web site at [cgj.nrc.ca](http://cgj.nrc.ca) on 1 October 2009.

**A. Strouth<sup>1</sup> and E. Eberhardt<sup>2</sup>** Geological Engineering – Earth and Ocean Sciences, 6339 Stores Rd., The University of British Columbia, Vancouver, BC V6T 1Z4, Canada.

<sup>1</sup>Present address: BGC Engineering Inc., 500-1045 Howe St., Vancouver, BC V6Z 2A9, Canada.

<sup>2</sup>Corresponding author (e-mail: [erik@eos.ubc.ca](mailto:erik@eos.ubc.ca)).

**Fig. 1.** Location of Afternoon Creek rockslide, east of Newhalem, Washington, showing outline of rockslide area. (Modified from figure 2 in Strouth et al. 2006, reproduced with permission of Landslides, Vol. 3, pp. 175–179, © 2006 Springer Science + Business Media.)

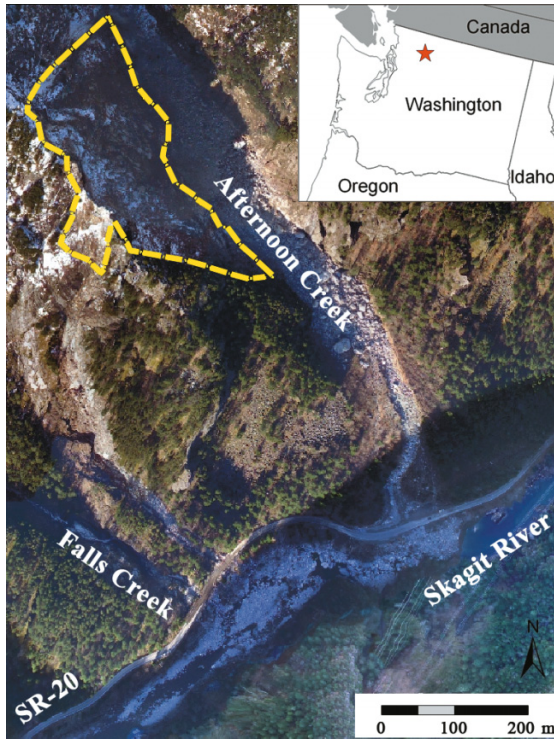
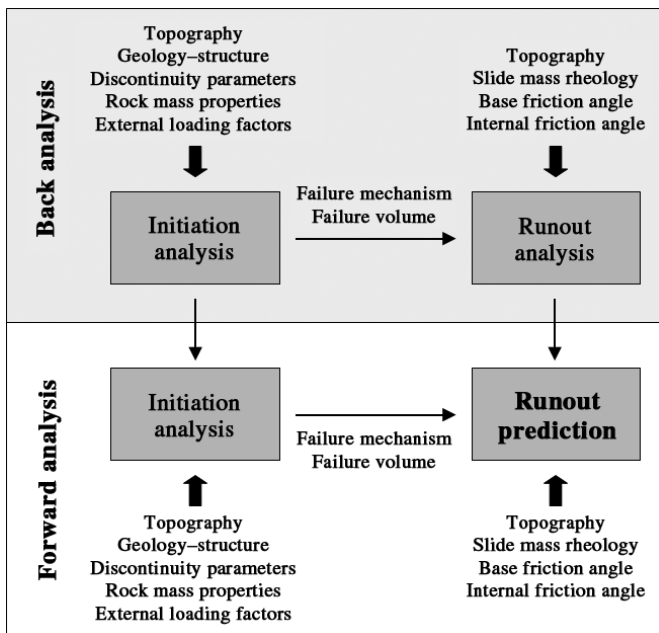
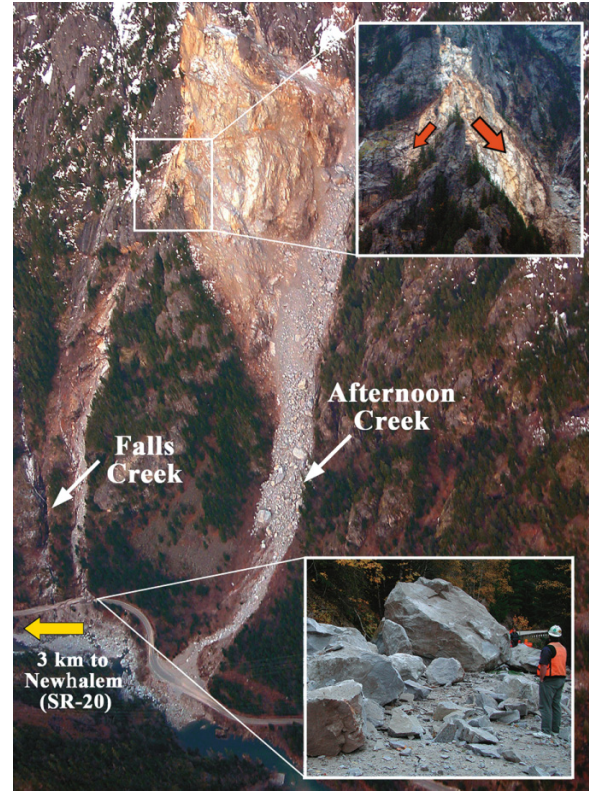


**Fig. 2.** Framework developed for integrated back and forward analysis of rock slope stability and potential rockslide runout paths, linking field data collection to different analysis types.



of future slope failures. This paper reports the findings of this study and the development of an integrated framework that links back and forward analyses of rockslide initiation and postfailure runout (Fig. 2). The methodology includes

**Fig. 3.** Overview of Afternoon Creek rockslide, showing size of blocks that impacted the state highway (lower inset photograph) and sharp ridge along the top of the source area controlling which of the two runout paths the failed material travelled down (upper inset photograph). (Modified from figure 1 in Strouth et al. 2006, reproduced with permission of Landslides, Vol. 3, pp. 175–179, © 2006 Springer Science + Business Media.)



the use of field mapping and laser scanning (light detection and ranging or LiDAR) to characterize the rock mass structure and discontinuity network and two-dimensional (2D) and three-dimensional (3D) distinct-element modelling (UDEEC and 3DEC; Itasca Consulting Group, Inc. 2003, 2004) to assess the rupture initiation process and the structural and topographic controls on the rockslide kinematics. These results were then used to guide analysis of postfailure motion, including rockslide runout path, distance, and velocities, using the dynamic rheological flow code DAN3D (McDougall and Hungr 2004).

**The 2003 Afternoon Creek rockslide**

The Afternoon Creek rockslide, described in detail by Strouth et al. (2006), occurred along a steep ridge adjacent to SR-20 near Newhalem, Washington, on 9 November 2003. Most of the rock avalanche debris (approximately 750 000 m<sup>3</sup>) travelled down into a narrow, steep-walled valley filled with older rockslide and rockfall debris (Afternoon Creek, Fig. 3). The distal edge of the material travelled approximately 300 m vertically and 500 m horizontally from the centre of the source area but did not reach the nearby highway. The resulting deposit was characterized as dry, very coarse granular material, largely composed of orthogneiss blocks ranging in diameter from 1 to 25 m (Fig. 4).

**Fig. 4.** Afternoon Creek rockslide and debris, showing (a) source area and deposit in Afternoon Creek and (b) size of blocks (person for scale).

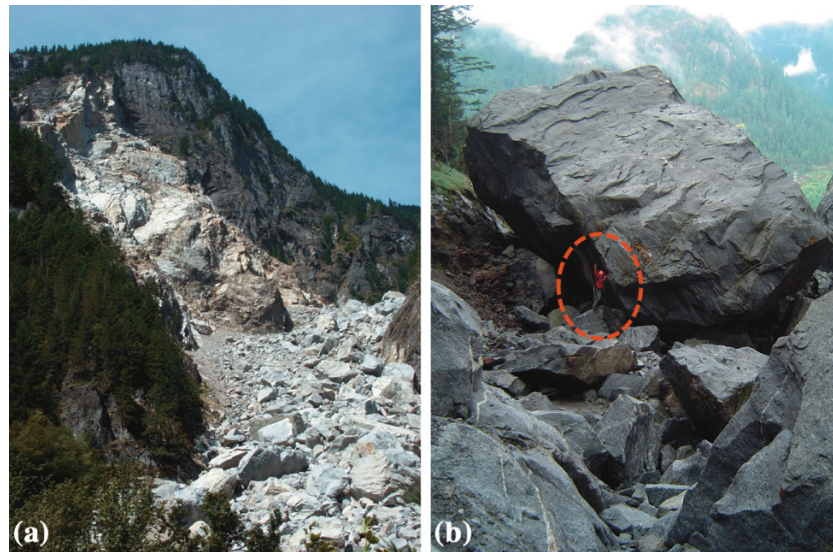
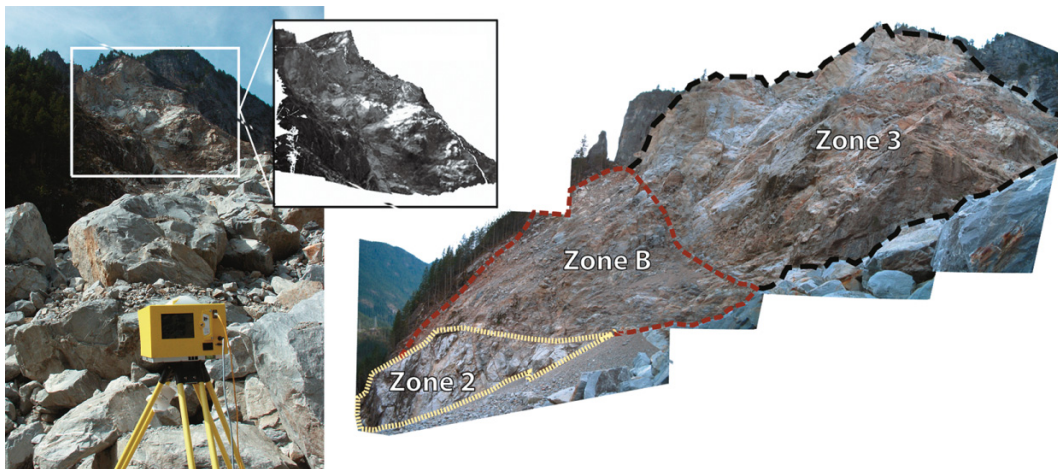


**Fig. 5.** (a) Terrestrial laser scanning (LiDAR) of the Afternoon Creek rockslide scarp. (b) Oblique photograph of the slide scarp, showing the structural domains defined through field mapping and LiDAR.



At the same time, the steep ridge from which the slide initiated acted as a topographic control that allowed a smaller amount (<10%) of the slide debris to travel down the back side of the ridge along a steeper descent path (Falls Creek, Fig. 3). This debris travelled more than 600 m in elevation downwards, impacting SR-20, an important route through the Cascade Mountains. Portions of the roadway and guard-rail were destroyed, and boulders up to 4 m in diameter were deposited on the road. This rockslide was followed by a series of smaller events over the next few months, and several large open fractures can still be observed, indicating that the rock slope still presents a danger due to potentially unstable material at the top of the ridge (Strouth et al. 2006).

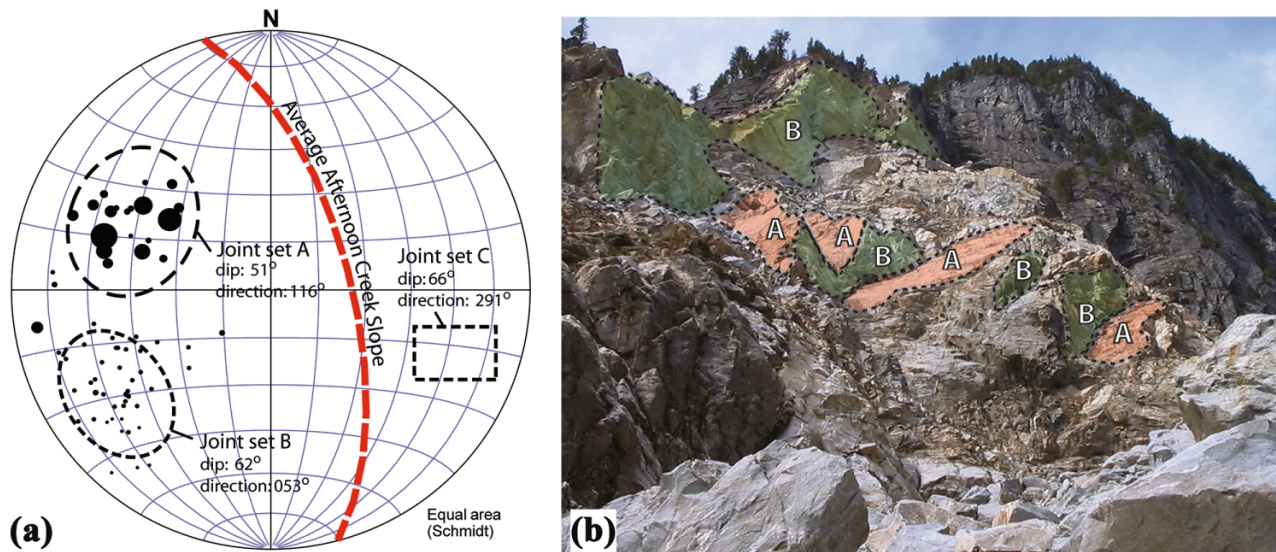
### Field investigations

Field investigations at the study site provided evidence of a history of rockfall, debrisflow, and rockslide activity at Afternoon Creek, although the 2003 event was the first large

rockslide on record. In assessing the in situ conditions prior to failure, Strouth et al. (2006) reported that glacial oversteepening of the slope, multiple cross-cutting fractures and shear zones, and decreased rock mass strength due to weathering and progressive failure (i.e., brittle fracturing of intact rock bridges) were key factors in conditioning the slope for failure. Heavy precipitation leading to high, joint water-pressure conditions is believed to have triggered the rockslide.

In carrying out the field investigation, mapping of the source area was hampered by the steep terrain and ever-present threat of rockfall. Only portions of the toe of the slide surface and its neighbouring outcrops could be mapped directly. However, this enabled several rock mass domains and joint sets to be qualitatively and quantitatively described through scanline mapping surveys. In addition, the field investigation allowed index tests to be performed to develop initial estimates of rock strength and joint roughness. Characterization of the discontinuity geometry, including orientation, spacing, and persistence, became the focus of the data collection program. To overcome the data challenges in the

**Fig. 6.** (a) Stereonet pole plot of LiDAR-determined discontinuities. Joint set orientation is the average orientation of poles included in the set. Pole size depicts relative joint persistence. (b) Oblique photograph showing joint sets A and B in structural domain zone 3, as identified in laser scanning data. Note that joint set C does not appear due to orientation bias.



upper slope, a terrestrial-based LiDAR scanner was used to collect discontinuity and rock mass characterization data.

#### LiDAR scanning and structural domains

Terrestrial LiDAR scans of the Afternoon Creek and Falls Creek slopes were performed with an Optech ILRIS-3D laser scanner from several vantage points ranging from 100 to 1 000 m from the slope face (Fig. 5a). The result of each laser scan is a 3D point cloud of the scanned surface from which discontinuity orientation, persistence, and spacing data were extracted. The point clouds were visualized and discontinuity data were extracted using Split-FX beta version 1.0 (Split Engineering LLC). After the point cloud is oriented and edited, the Split-FX software enables a polygonal surface mesh to be draped over the point cloud. Discontinuity surfaces are found by grouping neighbouring mesh triangles together based on the similarity of their vector normals and then fitting a plane through the points bounded by the grouped triangles. The discontinuity surface orientation, size, and roughness were recorded by the software and can be exported to any stereonet analysis package. The dimensions of the discontinuity surfaces and spacing between surfaces can be directly calculated from the coordinates of LiDAR points corresponding to the discontinuity surface.

From the LiDAR and outcrop mapping, the 2003 failure scarp was divided into three structural domains (zones 2, B, and 3) based on rock mass quality and structural pattern (Fig. 5b). Only zones B and 3 were directly involved in the 2003 rockslide. Zone B is the most highly fractured, lowest rock mass strength domain, with a geological strength index (GSI; Marinos and Hoek 2000) of 30–35. It is separated from zone 2 by the “base” shear zone and separated from zone 3 by the “tower” shear zone. Fracture intensity increases as proximity to the tower and base shear zones increases. Zone 3 is composed of massive, blocky gneiss (GSI = 60–65) with widely spaced and highly persistent jointing. From this zone, the 2003 failure released blocks up to 25 m in diameter (Fig. 4b).

Three principal joint sets were identified in zone 3, sets A, B, and C (Fig. 6). Joints in set A ( $116^{\circ}/51^{\circ}$ ) dip moderately out of the slope to the southeast, with an average persistence of 40 m and average spacing of approximately 5 m. Joints in set B ( $053^{\circ}/62^{\circ}$ ) dip moderately out of the slope to the northeast, making them the most important for global stability; their average persistence is 80 m and they have an average spacing of 14 m. Joint set C ( $291^{\circ}/66^{\circ}$ ) dips moderately into the slope to the northwest, with an average persistence of 30 m and average spacing of 8 m.

Kinematic analysis of the discontinuity data, based on stereonet projections (e.g., Fig. 6a) and field observations (Fig. 6b), indicates that planar sliding is feasible along joint set A, and wedge sliding is feasible along the intersection of joint sets A and B. Joint set C provides lateral release (and sometimes rear release) that allows planar and wedge sliding along joint sets A and B. In some cases, set B acts as a rear release for blocks sliding on set A. These release surfaces play an important role when simplifying the problem to a 2D cross section for numerical modelling purposes (as described later in the paper).

#### Rock-mass properties

The estimated compressive strength of the intact rock in structural domain zone 3 was 90 MPa, corresponding to grade R4 or “strong” rock (Hoek and Brown 1997). This was combined with the GSI value assigned to each structural domain to derive a set of rock-mass properties using the procedure outlined in Hoek and Brown (1997) and Hoek et al. (2002). The Mohr–Coulomb shear strength (friction angle and cohesion) and tensile strength were estimated using a linear best fit to the nonlinear Hoek–Brown strength envelope over a range of low confining pressures (see Hoek et al. 2002). These rock-mass properties were assigned to the intact blocks in the distinct-element models, thus treating them as an equivalent continuum to account for the strength-reducing effect of smaller scale discontinuities not explicitly represented in the models.

**Table 1.** Geometric and mechanical parameters derived for UDEC stability and failure initiation analysis.

(A) Geometric parameters					
	Joint set A	Joint set B	Tower shear	Base shear	
Dip	50°	61°	~ 85°E	~ 20°W	
Spacing (m)	10	25	na	na	
(B) Mechanical properties					
	Massive gneiss (zones 2 and 3)	Shear zone (zone B)			
Young's modulus (GPa)	24	2			
Poisson's ratio	0.2	0.2			
Density (kg/m <sup>3</sup> )	2650	2650			
Rock-mass cohesion (MPa)	2.0	0.5			
Rock-mass friction (°)	60	40			
Rock-mass tensile strength (kPa)	220	35			
Joint normal stiffness (GPa/m)	10	10			
Joint shear stiffness (GPa/m)	5	5			
Joint friction (°)	33	26			
(C) Damage-dependent properties					
	Initial state	Damage state 1	Damage state 2	Damage state 3	Damage state 4
Joint cohesion (kPa)	1000	500	100	10	0

Note: na, not applicable.

Joint sets A and B were explicitly included in the numerical models, requiring their properties to be treated separately. Estimates of discontinuity stiffness and strength were derived from published data of strength tests (Kulhawy 1975; Barton 1976) based on field observations of the joint characteristics (surface roughness, alteration, etc.). These values were verified and constrained during the numerical analysis (see Table 1). The joint friction angle required for the Afternoon Creek numerical modelling was an apparent value rather than a material property. The “dry” numerical models incorporated the basic friction angle for the material, the strength-reducing effect of pore-water pressure, and the strength-increasing effect of discontinuity roughness. The justification for this treatment is discussed in the section describing the back analysis performed. For joint cohesion, a range of values were tested to account for varying assumptions regarding the role of shear resistance provided by intact rock bridges. Fully persistent discontinuities with no infilling are often assumed to have zero cohesion, but many discontinuities are not fully persistent at the scale of the Afternoon Creek rock slope. Intact rock bridges add a component of shearing resistance that decreases with development of the rupture surface as fractures propagate and coalesce with the natural joints. As a starting point, initial values were based on those recommended by Wyllie and Mah (2004) for discontinuities in hard rock (cohesion ranging from 0 to 100 kPa). These were then adjusted for the field conditions at Afternoon Creek and decreased in increments from the maximum value to zero to simulate the propagation of joints in the numerical models (Table 1).

## Analysis approach

Although different analytical tools may be used to assess rockslide initiation and runout, they do not need to be

treated separately. Stead et al. (2006) proposed a “Total Slope Analysis Approach” in which advanced numerical models used to investigate rockslide initiation are further used to provide valuable information, such as deformation characteristics and kinematics prior to failure, relevant to the modelling of postfailure movement and dynamics. This approach was used to develop a framework for the hazard investigation at Afternoon Creek, linking back analyses of the 2003 rockslide and runout to forward predictive models. Doing so enabled results from each step to be used to provide mechanistic controls and parameter constraints for subsequent steps in the hazard assessment (Fig. 2), including the anticipated mode of rupture and the rock slope stability state (including its sensitivity to different environmental factors) to the potential extent, depth and volume of failure.

## Back analysis of the 2003 Afternoon Creek slope failure

### Stability and failure initiation

The stability analysis carried out for the 2003 Afternoon Creek rockslide involved parametric studies to better understand the prefailure stability state and its sensitivity to different internal and external factors and the resulting failure mechanism. The objective of these analyses was to provide understanding and model constraints to guide the development and interpretation of back analyses of the 3D postfailure runout behaviour and become a starting point for the forward analysis of the present-day hazard, anticipating the character, location, size, and effects of future rock-slope failures at Afternoon Creek (Fig. 2). For this case, it was important to determine whether failure would occur as a single extremely rapid event; multiple, smaller volume events; or a gradual, retrogressive, piecemeal disintegration of the unstable rock mass.

**Fig. 7.** Kinematic analysis showing the average and local slope orientations superimposed on a topographic map. Heavy contour lines in zone 3 show isopachs of rockslide thickness. Inset diagram shows stereonet projection of joint sets A and B, relative to the average and local slope face, and arrows indicate directions of planar (set A) and wedge (intersection of sets A and B) movement. CI, contour interval.

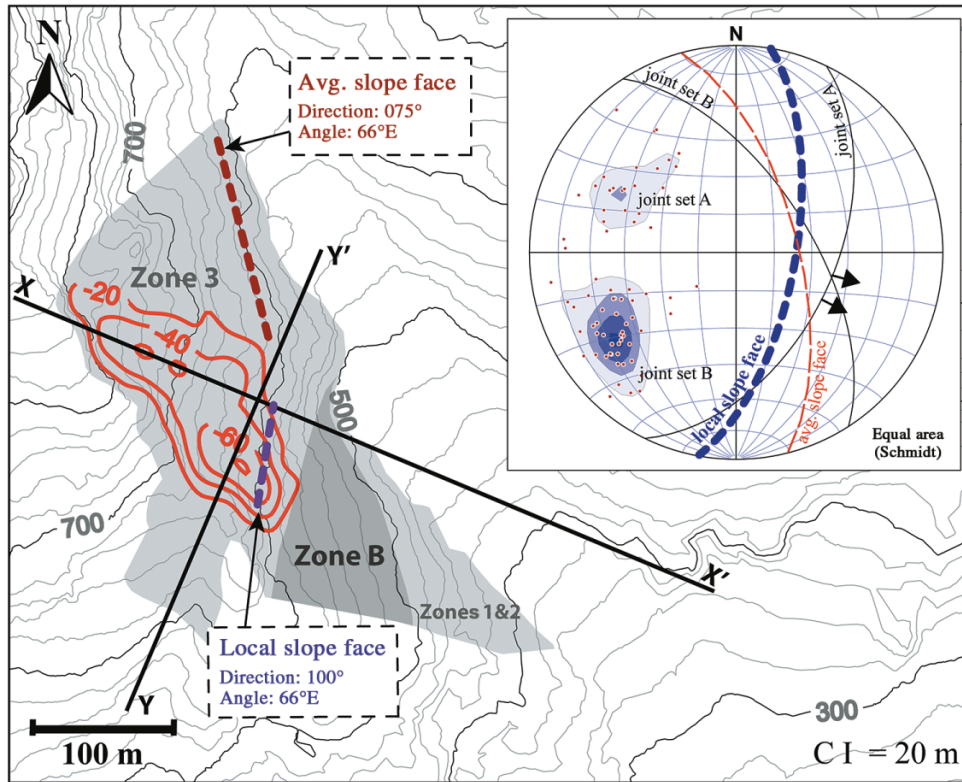
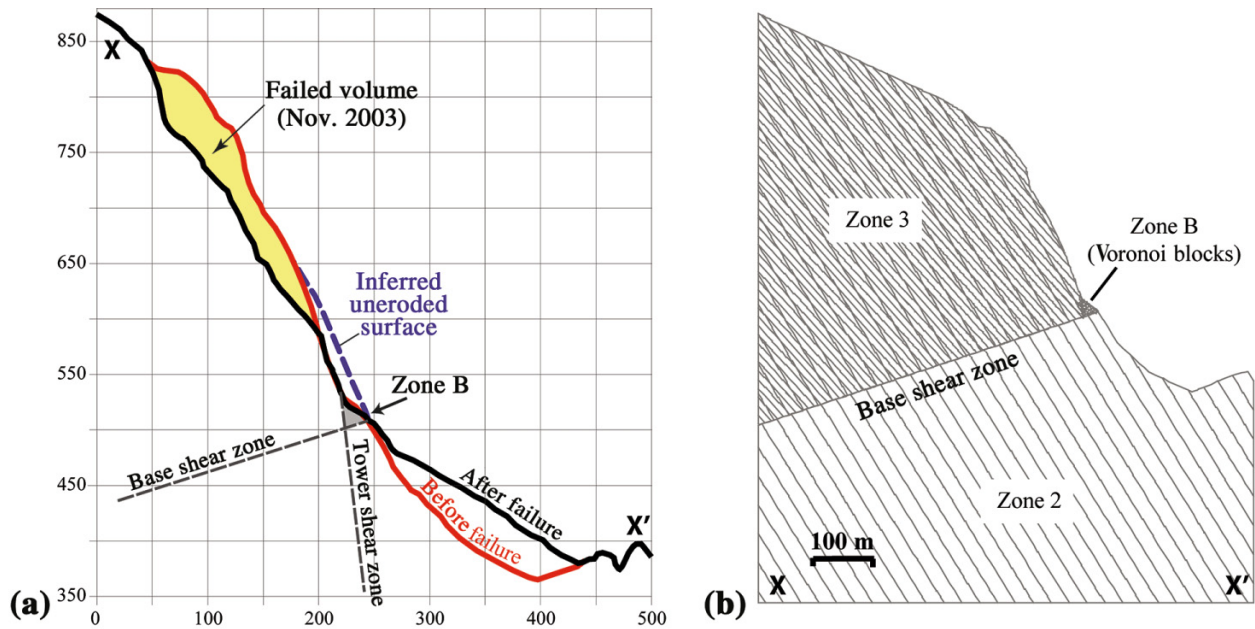


**Fig. 8.** (a) Cross section X–X' showing the prefailure and postfailure topography related to the 2003 Afternoon Creek rockslide. (b) Corresponding 2D distinct-element model.



Several analysis techniques were used to exploit the advantages and benefits of each technique, including kinematic, limit equilibrium, and 2D and 3D distinct-element modelling. Only the kinematic and numerical modelling results are reported here for conciseness (see Strouth 2006 for

limit equilibrium analysis). The distinct-element method (Hart 1993) is well suited to rock-slope stability problems, modelling the problem domain as an assemblage of deformable blocks and accounting for complex nonlinear interactions between the blocks (i.e., slip and (or) opening–closing

Fig. 9. Modelling procedure followed for back analysis of the Afternoon Creek rock-slope failure.

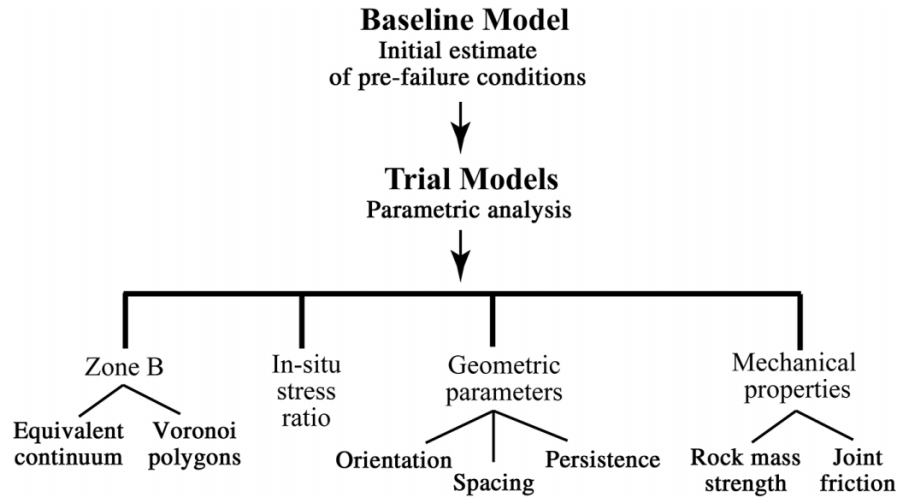
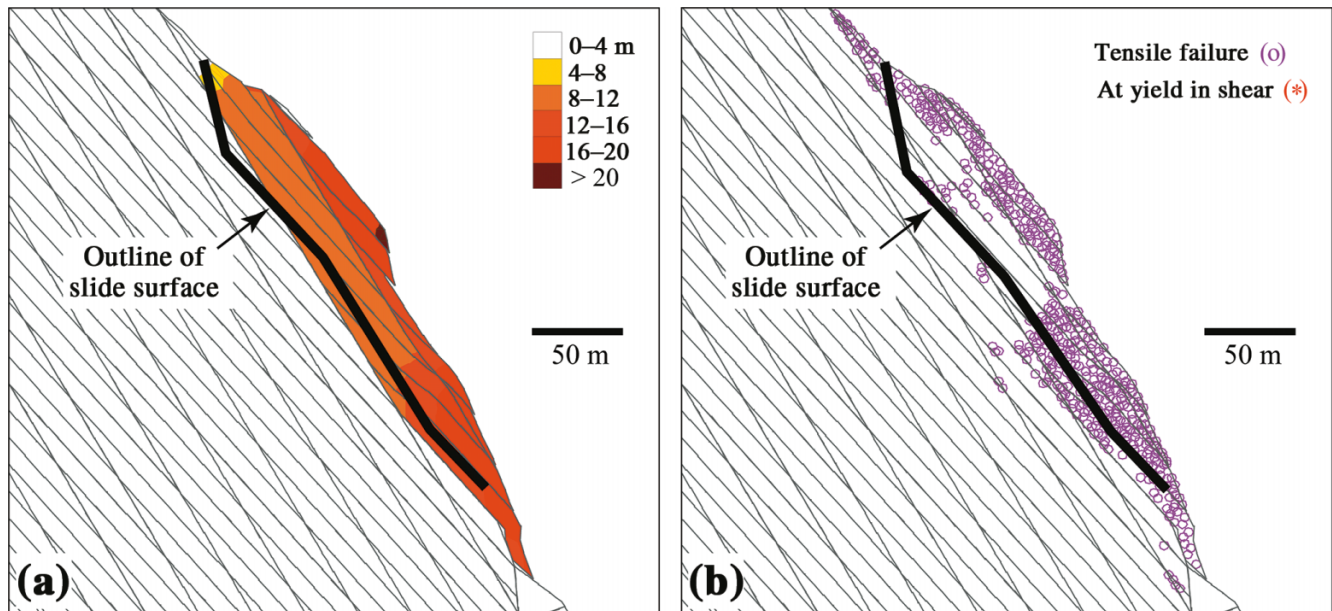


Fig. 10. Two-dimensional UDEC results of rock slope failure at damage state 4 (see Table 1), showing (a) horizontal displacement contours and (b) plasticity indicators.



along discontinuities). Pore-water pressures were not explicitly included in the distinct-element models, since their magnitudes could not be adequately constrained due to the discontinuous nature of the permeability network (intact orthogneiss blocks and rock bridges were assumed to be effectively impervious). Instead, they were treated implicitly in the backcalculated discontinuity strength parameters.

#### Kinematic analysis

Results from the kinematic analysis suggested that a variation in slope trend along the Afternoon Creek ridge may have influenced the location of failure (Fig. 7). The slope direction varies due to a contrast in the weathering resistance of the rock in the different structural domains. The highly fractured zone B domain weathers more easily than the surrounding massive, more competent zones 2 and 3 domains. Weathering of zone B created a notch in the slope that in turn appears to play an important control in destabilizing the slope.

Specifically, in terms of the slope kinematics, the change in local slope direction to  $100^\circ$  near the boundary of zones B and 3 from the average slope face direction of approximately  $075^\circ$  enables wedge sliding along the intersection of joint sets A and B and planar sliding along joint set A (Fig. 7).

#### UDEC analysis

The topographic and geological cross section used to develop the 2D distinct-element models was taken along the direction of movement (X-X' in Fig. 7). It should be noted that the lower sections of the slide mass just above zone B, i.e., those blocks that failed first, likely moved oblique to this in a more easterly direction. Figure 8 shows the corresponding cross section and 2D UDEC model, which was used to develop a baseline case representing the initial best estimates of the pre-failure conditions to which all subsequent models were compared. These trial models addressed

**Fig. 11.** Photograph showing present-day subvertical open tension cracks behind the back scarp of the 2003 Afternoon Creek rock-slide.

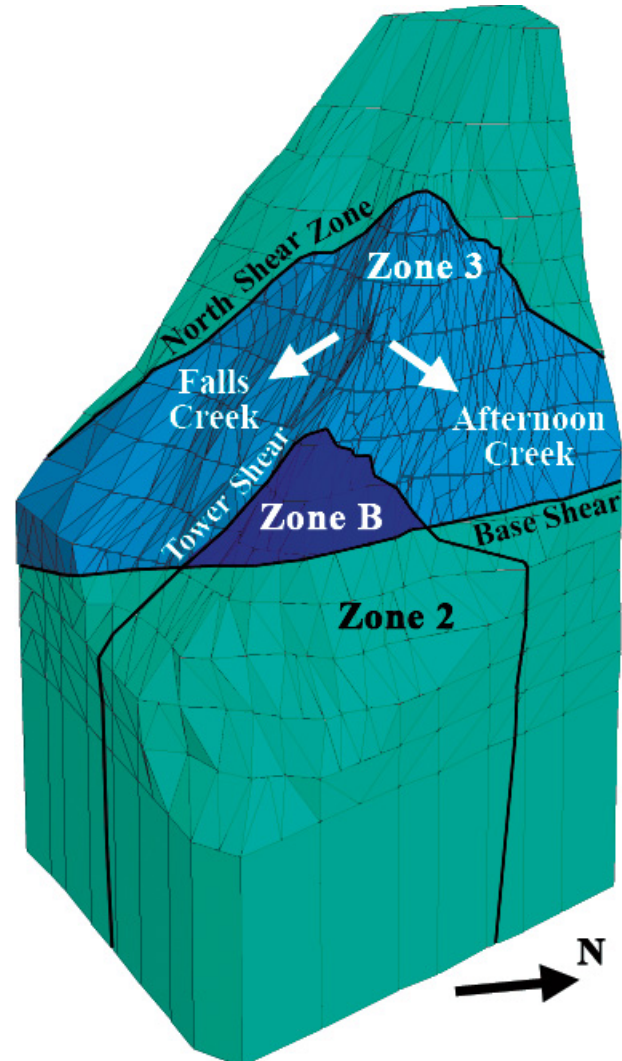


the uncertainty associated with several key input parameters and assumptions (Fig. 9), including modelling zone B as either a weak equivalent continuum or a network of randomly sized polygonal blocks (Voronoi blocks); varying the in situ stresses defined in terms of the ratio of the horizontal stress to the vertical stress ( $K = 0.5, 1, \text{ and } 2$ ); varying the dip, spacing, and persistence of joint sets A and B and dips of the tower and base shear zones; and varying the rock mass friction, cohesion, and tensile strength properties. The finite-difference mesh used to discretize the deformable blocks was refined so that smaller elements were assigned to areas where high stress concentrations and strain gradients were expected to develop. A Mohr–Coulomb elastoplastic constitutive model was applied throughout the problem domain.

After time stepping each model to an initial equilibrium, the joint cohesive strength was incrementally decreased in a series of damage states (Table 1), following the example of Eberhardt et al. (2004), to simulate the time-dependent weakening and progressive failure of intact rock bridges along the modelled discontinuities. The model response for each damage state was then monitored for either equilibrium or rupture and movement using plots of unbalanced forces, displacement, velocity, and element plasticity state.

Results from the baseline and trial cases were similar, with failure occurring in a biplanar manner with the upper

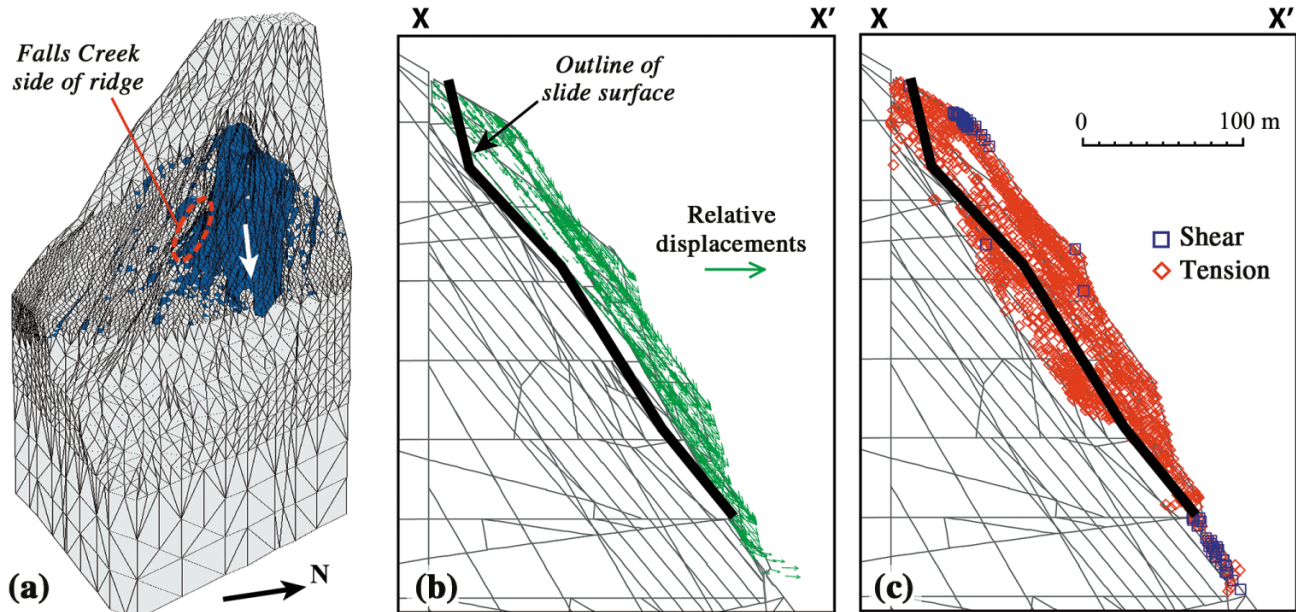
**Fig. 12.** 3DEC model of Afternoon Creek.



sliding surface predominantly following joint set B and the toe of the failure sliding out on the shallower dipping joint set A (Fig. 10a). This agrees with field observations. Also in agreement was that the rupture surface did not develop through zone B but above it in zone 3. Although zone B is composed of weaker rock, the critical joint planes (sets A and B) do not persist through it, resulting in the rupture surface favouring a path that daylights above zone B (Fig. 10a). This was the case whether zone B was modelled as a weak equivalent continuum or as a system of small Voronoi blocks. Plasticity indicators (Fig. 10b) showed that tensile yield was more dominant than shear yield in the joint-bounded blocks, largely driven by displacements initiated at the toe of the slope. This is consistent with the brittle nature of the rock mass and was clearly evident in the surface characteristics of the rock blocks in the slide debris (e.g., note the faceted surface of the large block in Fig. 4b). A small concentration of tensile yield indicators was also observed to develop at the top of the slope behind the back scarp, which coincides with vertical columns of rock separated from the main rock mass by deep tension cracks (Fig. 11), evidence of the high tensile stresses that acted in this region of the slope.



**Fig. 13.** 3DEC modelling results. (a) Three-dimensional view of yielded elements on surface. Shaded elements indicate yield in tension. The white arrow indicates the direction of movement of the yielded blocks on the Afternoon Creek side of the model. The broken circle shows yielded elements on the Falls Creek side of the ridge. (b) Cross section through the 3-D model comparing block displacements and the outline of the Afternoon Creek rockslide failure surface. (c) Tensile and shear plasticity indicators for the comparison shown in (b). See Fig. 7 for alignment of section X–X'.



It should be noted that the results in Fig. 10 are those for the baseline case where zone B was modelled as a weak equivalent continuum. This case provided the best results, although interestingly no significant deviations from the baseline case were observed for the different trial cases. In fact, the similarity in response between the baseline and trial models and their agreement with the actual event in terms of failure mechanism and volume of material displaced help to establish a high degree of confidence in the models. Based on the common elements between the different simulations, it can be established that the path along which the rupture surface developed is largely limited to the two dominant joint sets mapped, namely the moderately dipping set (A) along which sliding at the toe is enabled, and the steeper set (B) that helps to form a rear release surface. Their explicit inclusion in the UDEC simulations likewise dominates the modelled response. Although these joints are persistent, they are not fully persistent, resulting in a stepped sliding surface that exploits the connectivity of the two joint sets together with the simulated destruction of intact rock bridges. For the baseline case, development of the rupture surface coincided with damage state 2 (see Table 1), i.e., when the joint cohesion was reduced to 100 kPa. Sliding continued on the same planar surfaces after the joint cohesion was reduced to damage state 3 with failure coinciding with damage state 4.

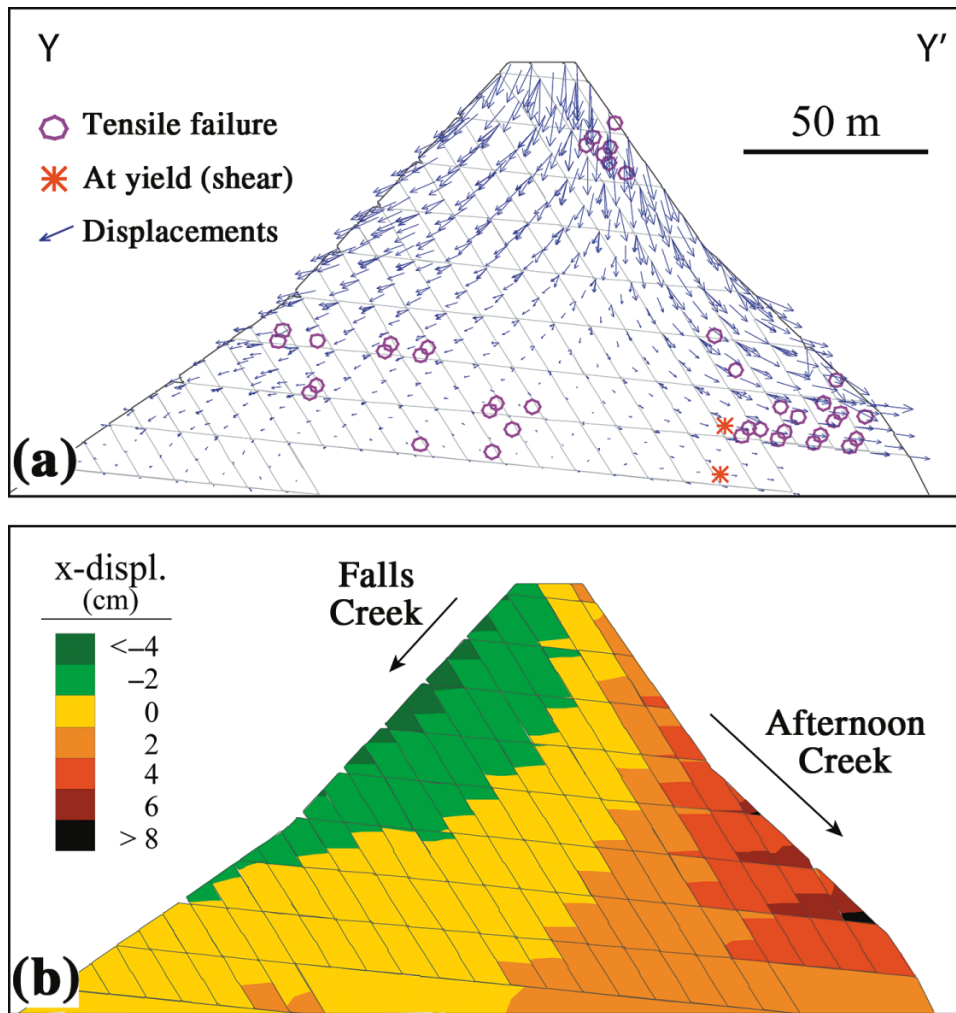
### 3DEC analysis

Several issues related to the slope failure process were left unresolved by the 2D analysis, including whether the failure occurred in stages or as a single-volume event and the differences in movement direction between the upper and lower sections of the rockslide. For this, 3D distinct-element models were developed using the commercial code 3DEC

(Itasca Consulting Group, Inc. 2003) following the same methodology as that for the 2D UDEC models. The 3D model was generated using a prefailure digital elevation model (DEM) to define the modelled surface topography and the mapped discontinuity data to create convex polyhedral blocks to define the initial rock mass kinematic conditions (Fig. 12). An accurate representation of the topography was deemed necessary to properly capture its influence on deformation and failure; small irregularities in the topography were smoothed to simplify the finite-difference mesh-generation process and speed up solution run times. The 3DEC model included both the discontinuity characteristics defined for each of the mapped zones (joint sets A and B) and three of the major shear zones mapped in the slope (Fig. 12). Zone B was modelled as a weak, equivalent continuum as was done in the UDEC simulations, assigning smaller elements to improve on accuracy given the expected plastic yielding and high-strain gradients expected to occur in this region of the model. Similar to the UDEC base model, the in situ stresses were set to  $K = 1$ . The material properties for the 3DEC analysis were taken directly from the UDEC analysis and parametric study (Table 1).

After stress initialization, zones B and 3 were changed to Mohr–Coulomb elastoplastic materials, and the joint cohesion was incrementally decreased through a series of damage states to simulate strength degradation along the joints due to the progressive failure of intact rock bridges (as was done for the 2D UDEC simulations; see Table 1). The subsequent results (Fig. 13) showed that the 3D mode, extent, and volume of failure were similar to those approximated in 2D, again closely agreeing with observations made in the field. The failure mechanism of the 3DEC model indicated sliding on discontinuity surfaces that daylight above zone B, with the rupture surface stepping up along joint sets A

**Fig. 14.** UDEC modelling of failure mechanism on Falls Creek side of ridge, showing (a) plasticity indicators and displacement vectors and (b) horizontal displacement (*x*-displ.) contours. See Fig. 7 for alignment of section Y–Y’.

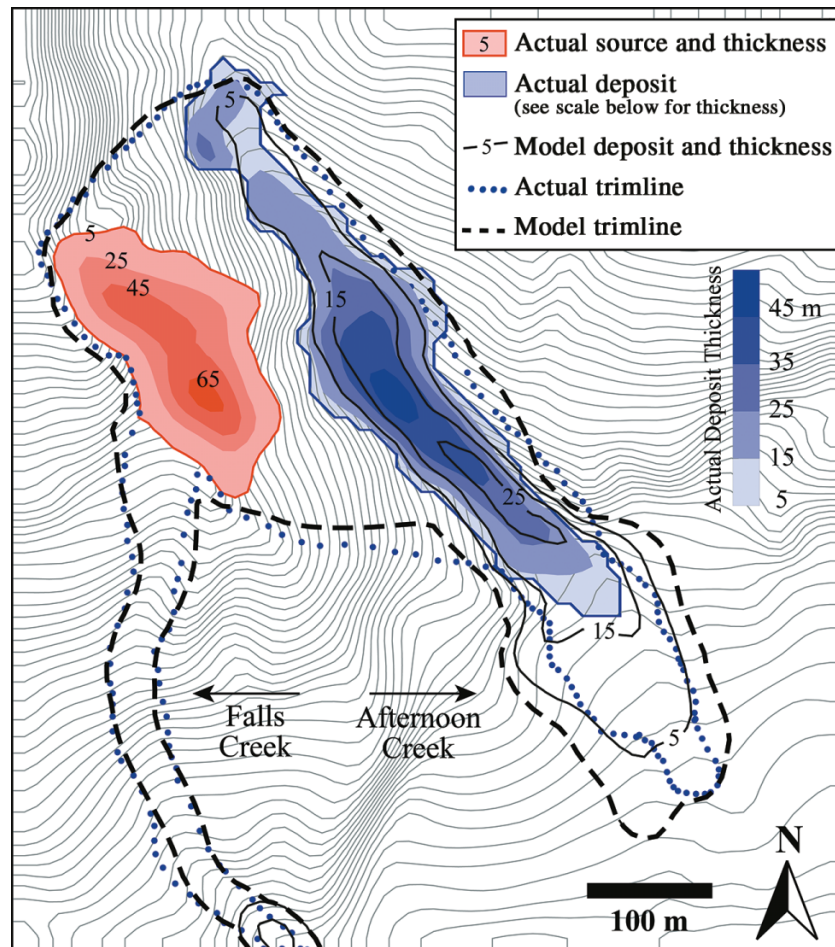


and B (Fig. 13*b*). Sliding occurred primarily in the dip direction of joint set A; joint set B provided rear release for the sliding blocks. The uniform movement of the failed blocks in the model, coupled with the translational, planar nature of the rockslide, suggests that the volume on the Afternoon Creek side of the ridge was released as a single event (Figs. 10*a*, 13*b*). Tensile yielding occurred extensively in the rock mass above the sliding planes, and the plastic yield indicators clearly show the extent of the rockslide volume both on surface (Fig. 13*a*) and at depth (Fig. 13*b*). On the surface, the single-event volume extends longitudinally from the top of zone B to the north shear zone and laterally from the ridge crest to a topographic low in the northern extent of Afternoon Creek (Fig. 13*a*). The extent of the rockslide volume in the 3DEC model closely matches the mapped extent of the 2003 Afternoon Creek rockslide and points to the failure being strongly controlled by both the ridge topography and the two identified joint sets.

The key added feature of the 3D model, relative to the 2D model, was the inclusion of the 3D ridge topography. The results in Fig. 13*a* (see circled area) showed that a small number of yielded elements occur on the Falls Creek side

of the ridge, opposite that of the main rockslide. This is an important consideration given that the slide debris that actually impacted the highway travelled down the Falls Creek side of the ridge. The 3D model, however, was deficient in that computing limitations required relatively large block sizes, compared to those in situ, that imposed kinematic restrictions in the modelled response in terms of explicitly showing block movements entering the Falls Creek travel path. To examine the mechanism on the Falls Creek side of the ridge in more detail, a series of 2D UDEC models based on the 3DEC results were constructed along cross section Y–Y’ (see Fig. 7 for plan-view location). These models (Fig. 14) explored different kinematic influences imposed by joint sets A and B on the opposite side of the ridge, including translational sliding and toppling. The results showed that, although translational movements of blocks on the Falls Creek side of the ridge may have partly contributed to slide debris entering Falls Creek, pervasive planar or wedge sliding was unlikely. Instead, toppling of individual columns into Falls Creek appeared to be a more likely mechanism (Fig. 14), one that can be seen in the remaining rock above the slide scarp and along the ridge (Fig. 11).

**Fig. 15.** DAN3D runout analysis of the 2003 Afternoon Creek rockslide, showing comparison between modelled and mapped trimlines and between modelled deposit thickness and that derived from before and after digital elevation models.



### Runout analysis

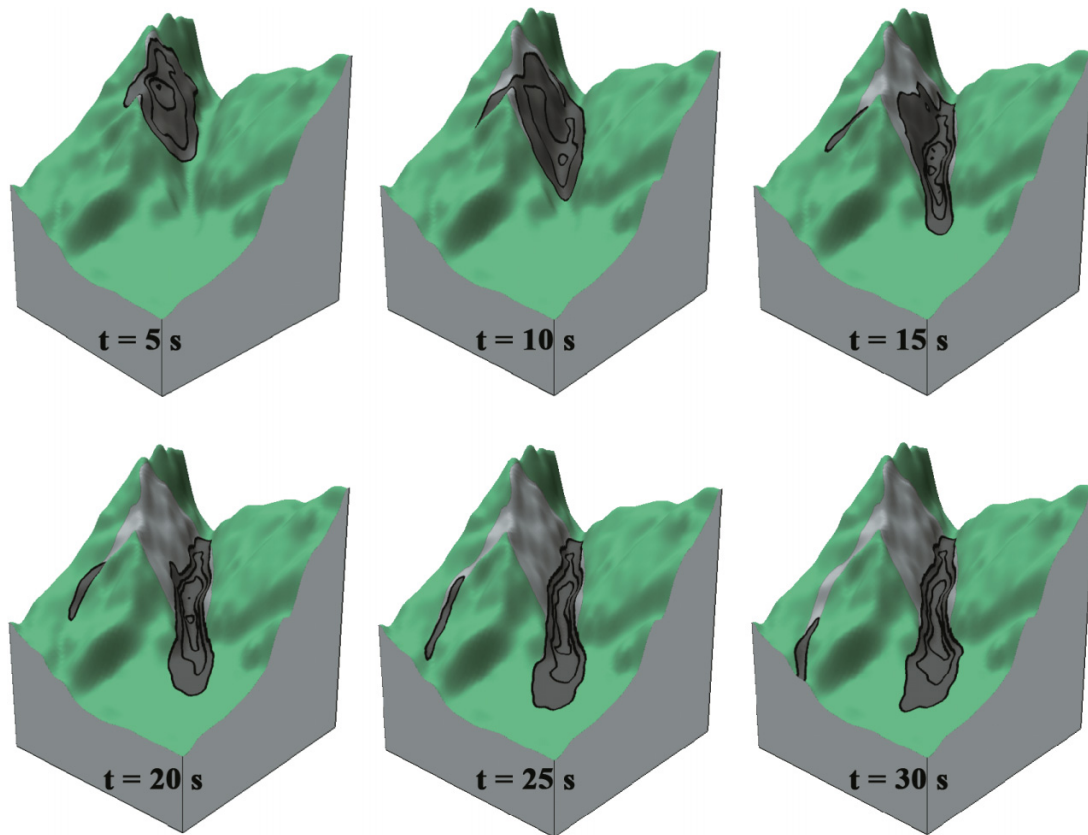
Runout simulations were undertaken using the results of the UDEC and 3DEC stability analyses to back analyze and quantitatively assess the travel path, distance, and deposit characteristics of the 2003 Afternoon Creek rockslide (Fig. 2). Again, although the leading edge of the rockslide travelled more than several hundred metres into Afternoon Creek, it did not reach the highway. Only a small volume that travelled in the opposite direction down Falls Creek impacted the road. Thus, the runout back analysis formed an important step in providing information that could be used to anticipate the effects of future rockslides from the ridge above Afternoon Creek.

For this, the numerical dynamic–rheological flow code DAN3D (McDougall and Hungr 2004) was used. DAN3D is based on a Lagrangian smoothed particle hydrodynamics (SPH) formulation and allows for the modelling of complex, multidirectional landslide movement over equally complex 3D terrain. McDougall et al. (2008) have shown through back analyses of a number of landslide case histories the ability of such codes to consistently simulate actual events. The information required by the DAN3D analysis includes a DEM of the runout path, the volume and initial location of the sliding mass, an appropriate rheological model, and constitutive properties of the runout material and runout

path. In the simulations performed here, the runout path and source volume were derived by comparing the topography of Afternoon Creek before and after the event. The material properties were initially estimated and then calibrated using runout characteristics mapped in the field.

The source zone and rock-avalanche deposit were identified and delineated on aerial photographs and through field mapping and used to quantify the thicknesses, areas, and volumes of the source zone and deposit. The estimated source volume was approximately 641 000 m<sup>3</sup>, and the volume of the deposit was approximately 868 000 m<sup>3</sup>, corresponding to a 35% bulking caused by fragmentation of the rockslide material. A dry frictional rheology was assumed for this analysis based on the experience of Hungr and Evans (1996), McDougall and Hungr (2004), and others in modelling large rockslide runouts. This requires estimates of the internal friction angle of the runout material and basal friction angle. These parameters, once calibrated, are considered apparent (or bulk properties) rather than true physical material parameters (McDougall and Hungr 2004). The internal bulk friction angle used to derive the tangential stress coefficients (Hungr 1995) can be related to the angle of repose, which was measured in the field. The basal bulk friction angle is the average friction angle along the entire runout path between the path interface with the moving

**Fig. 16.** Time ( $t$ ) snapshots from DAN3D runout analysis, showing majority of slide debris entering Afternoon Creek but with a small volume splaying off and entering Falls Creek.



mass. This value depends on the hard-to-quantify effects of several variables, including composition of the path and moving mass and the velocity of the moving mass. Aerial photographs that predate the 2003 rockslide show that the Afternoon Creek valley was a bedrock channel filled with colluvium mostly made up of blocky orthogneiss boulders and fragmented rock. The average angle of repose of the deposit is approximately  $37^\circ$ . This was the initial estimate for both the basal and internal friction angles.

Based on the results of the UDEC and 3DEC analyses, the entire source volume was modelled as being released as a single event (as opposed to multiple small-volume retrogressing events). After several calibration runs, the frictional strength parameters that most closely reproduced the physical characteristics of the actual runout event were  $37^\circ$  for the bulk basal friction angle and  $40^\circ$  for the bulk internal friction angle. The results of the analysis resembled the actual event in a number of ways: the shape of the deposits and reach of the leading edge of the debris are similar, and the model trimline closely matched the actual trimline (Fig. 15). The trimline is defined here as the boundary along which the slide debris scoured away the vegetation, marking its travel path. In addition, most of the simulated debris is deposited in the narrow section of Afternoon Creek, but a small volume does travel down Falls Creek, as was the case in the actual slide (Fig. 16).

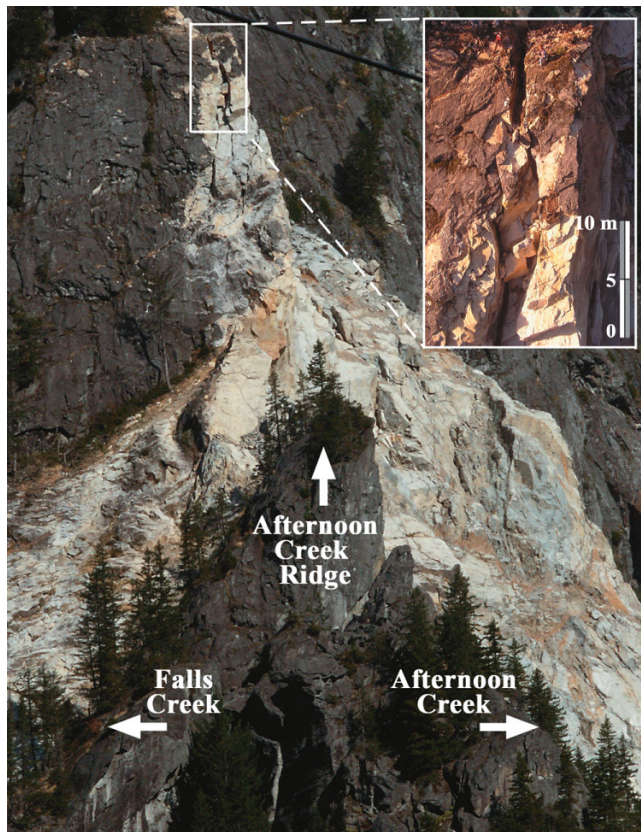
The key differences between the calibrated model and the actual event were that the centre of the modelled mass travelled somewhat farther than the actual runout and that the

modelled debris showed more spreading upon exiting the narrow Afternoon Creek canyon (Fig. 15). One reason for these differences is the assumption (required by DAN3D) that the entire source volume fragments immediately at the start point of the model simulation. This results in higher initial internal pressures of the source volume in the model and therefore increased dispersion. Differences can also be attributed to the assumption of an average basal friction value along the entire path, instead of one that varies as the debris moves from the slope to the boulder-filled Afternoon Creek canyon to the finer grained Afternoon Creek fan at the end of the runout path. Despite these differences and the numerous simplifying assumptions made in the model, the DAN3D results produced an excellent match to the actual event, thereby providing confidence in the model and the overall methodology employed.

### Use of calibrated models for forward analysis of hazard posed by future rockslide events

The calibrated models and constrained estimates of the failure volume and mechanical properties and the understanding of the operative failure and runout mechanisms for the 2003 rockslide were subsequently used to guide a hazard assessment for the present-day rock slope (Fig. 2). For this, the runout analysis is perhaps the most important component of the hazard assessment, as it can be used to predict the effects of a future rockslide with respect to the likelihood of it

**Fig. 17.** Present-day conditions above Afternoon Creek and Falls Creek, showing large tension cracks and unstable rock columns above the ridge.



reaching the SR-20 highway, including the impact area, velocity, and deposit depth. However, before an accurate run-out analysis can be completed, it is necessary to locate and accurately estimate the volume of the rockslide source (McDougall and Hungr 2004).

#### Forward analysis of potential rock-slope failure

Visual inspection of the Afternoon Creek ridge indicates that there is a significant likelihood of another event originating from the crest above the 2003 rockslide scarp. Most striking is a number of long tension cracks that have the potential to enable toppling of individual rock columns (Fig. 17). In addition, there still appears to be the potential for planar or wedge sliding along joint set A because of the intersection of joints in set A with those in set B. To identify the operative failure mechanisms and determine how these may affect the volume of failed material and its run-out, further UDEC modelling was carried out. Cross section X-X' was again used as a basis for the UDEC analysis but modified to match the post-2003 topographic profile (Fig. 18a). The mechanical properties that had been calibrated during the back analysis were used. These are the same as those reported in Table 1 except that the joint friction angle was reduced to  $28^\circ$  to better promote sliding on joint set A. Several variations in orientation and persistence of joint set B were also tested to ensure that the resulting rockslide volumes predicted included most likely and worst case scenario outcomes.

The UDEC results showed that another rockslide event at Afternoon Creek was possible and would incorporate the ridge and crest of the oversteepened scarp and (or) sliding blocks in the central portion of the slope (Fig. 18b). The steeper joint set B was seen to provide rear release for the slide mass but also helped limit the depth of the rupture surface and retrogression of the crest. Such an event would be expected to be extremely rapid, similar to the 2003 Afternoon Creek event, due to the brittle nature of the rock mass, as evidenced by the predominance of tensile failure in the UDEC model (Fig. 18b). Based on projections of the 2D UDEC results to adjacent regions with similar topographic relief in the 3D DEM, the maximum volume of the failure along the ridge would be approximately  $100\,000\text{ m}^3$  (Fig. 18c); however, it is unlikely that the entire volume would fail simultaneously due to the toppling and wedge failure mechanism expected in this part of the slope. The maximum volume for the translational slide in the central portion of the slope would be on the order of  $300\,000\text{ m}^3$  (Fig. 18c); here, the entire volume has the potential to occur as a single event. This mechanism is equivalent to the failure mechanism observed in the UDEC models of the 2003 Afternoon Creek event.

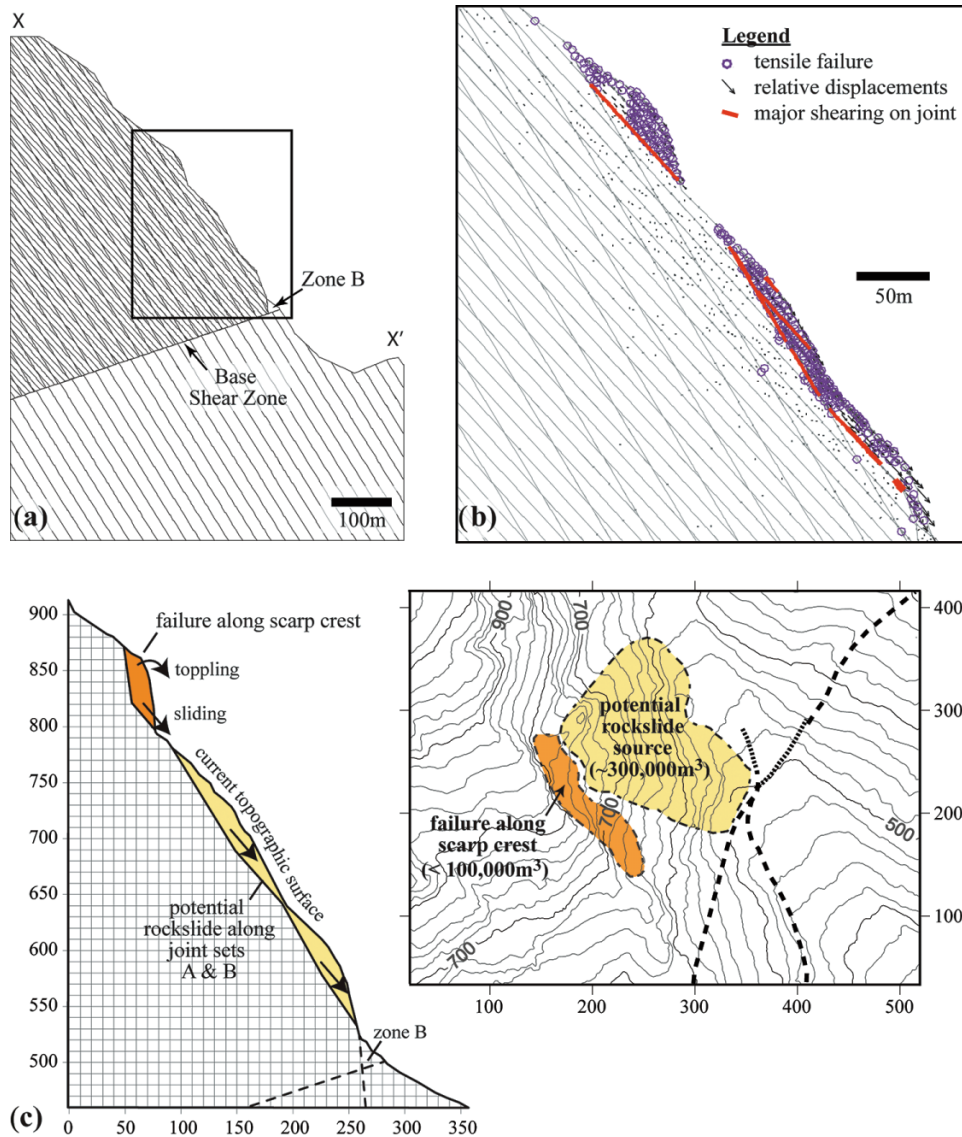
#### Forward analysis of potential rockslide runout

Due to topographic constraints, rockslide debris from the central portion of the slope would be restricted to the Afternoon Creek travel path. Translational sliding of this part of the rock mass is essentially a continuation of the November 2003 event except with a considerably smaller source volume. In contrast, sources originating near the crest of the slope as before have the potential to send debris down both the Falls Creek and Afternoon Creek sides of the ridge. Toppling of rock columns above the crest is considered the most likely event to occur, given the highly developed state of present-day tension cracks. The volume that would be involved in the toppling of a single column of rock is approximately  $1000\text{ m}^3$ . Kinematically, it appears that the toppling motion would be in the direction of Afternoon Creek; however, it may be possible for parts of the toppled column or associated rockfall to land on the opposite side of the ridge and travel down the steeper Falls Creek runout path.

The forward runout analysis carried out included both source zones identified through the UDEC modelling (Fig. 18c) but treated them separately. The results of the DAN3D back analysis of the 2003 rockslide runout were used to provide understanding of the rheology and estimates of the constitutive properties of the runout path and failed mass, including friction parameters (basal bulk friction =  $37^\circ$ , internal bulk friction =  $40^\circ$ ) and bulking ratio of the source volume (1.35). Hungr (1995) recommended the use of backcalculated properties where possible when performing a forward runout analysis. Variations included reducing the internal bulk friction value by 10% and increasing the bulking ratio by 50% as worst case scenarios. Other inputs varied for the runout assessment included the source volumes determined through the UDEC forward analysis. The runout path was created based on a DEM of the present-day 3D topographic surface. All runout simulations used the frictional rheological model.

The first scenario tested involved the larger of the two po-

**Fig. 18.** (a) UDEC model for forward analysis of present-day conditions at afternoon Creek. (b) Predictive UDEC results. (c) Estimation of potential failed volume derived from UDEC results and subsequently used for runout analysis. Graph scales and map contours in metres.



tential rockslide sources, namely that of a 300 000 m<sup>3</sup> rockslide originating from the central portion of the slope. As this is below the dividing ridge, the models each show all of the material entering Afternoon Creek and then stopping before impacting the SR-20 highway. The worst case scenario results are presented in Fig. 19. Here, a thin layer of debris (less than 5 m thick) travels onto the Afternoon Creek fan, but the leading edge of the deposit stops more than 100 m short of the highway (Fig. 19a). The predicted runout decreases to 200 m short of the highway when using the backcalculated input parameters instead of the worst case scenario parameters. The leading edge of the material comes to an abrupt stop, decelerating over a very short distance. The maximum velocity reached along most areas of the travel path was between 15 and 25 m/s for the different model variations. The overall maximum velocity was slightly greater than 45 m/s (Fig. 19b). Based on these results, it can be concluded that rockslide debris originating

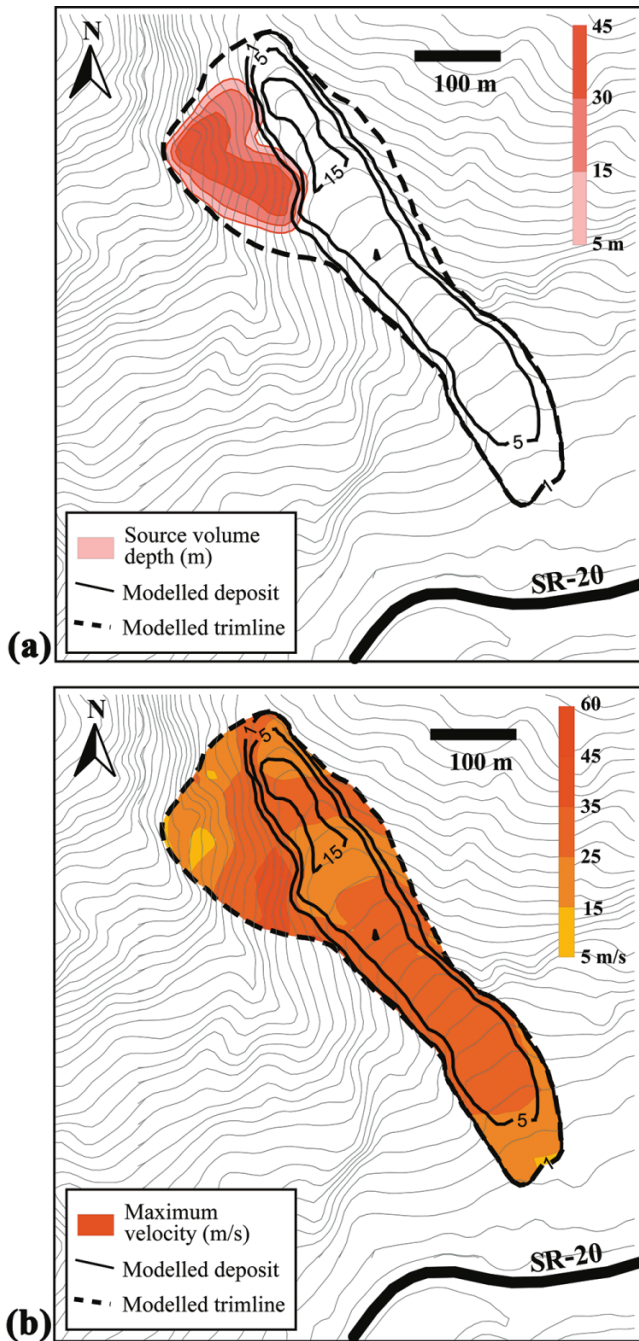
from the central portion of the slope is unlikely to reach SR-20 via Afternoon Creek.

The second scenario tested examined the other potential rockslide source involving a volume of approximately 100 000 m<sup>3</sup> at the crest of the ridge. Again, assuming the worst case scenario parameters, the model results show most of the material entering and travelling down Afternoon Creek but coming to rest 150 m short of the highway (Fig. 20). However, the model also shows 2%–3% of the total source volume separating from the main mass, entering the Falls Creek runout path, and impacting the highway (Fig. 20). The same result was obtained for the baseline models using less conservative input values but with a smaller volume impacting the highway.

**Summary of hazard assessment and remedial measures**

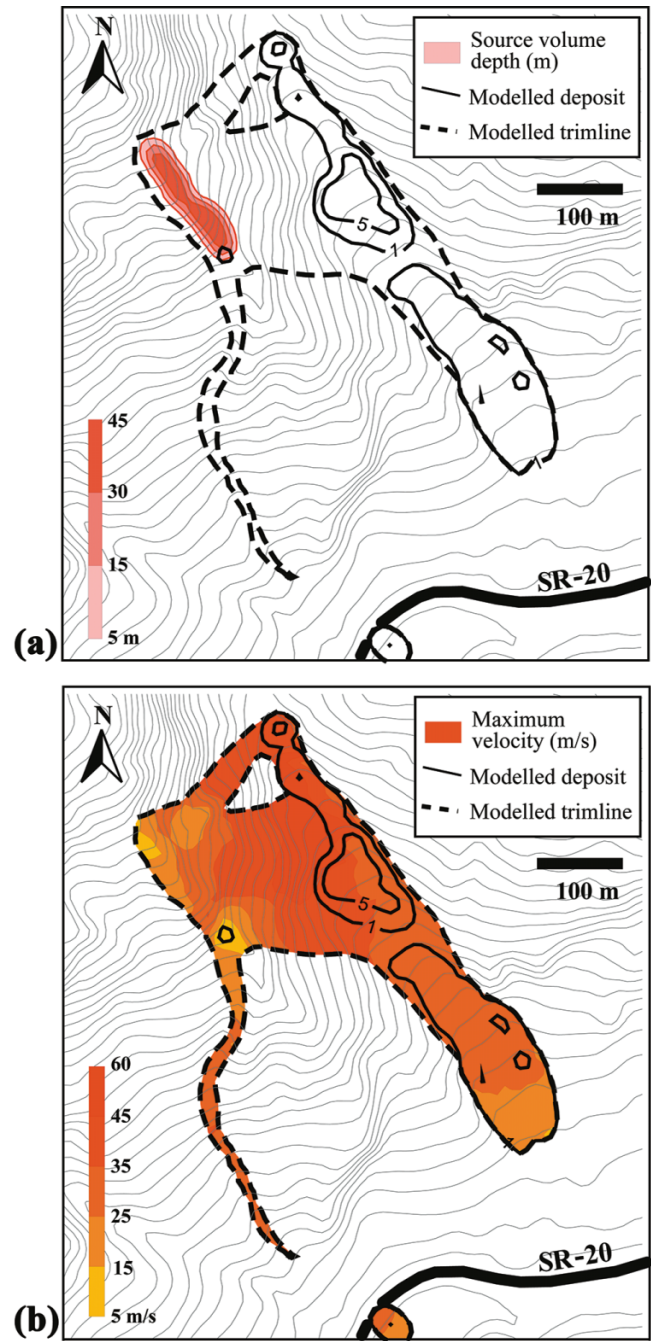
The runout models show that it is unlikely that a large-volume rockslide originating from the crest or middle of the

**Fig. 19.** DAN3D forward analysis and runout assessment for a rockslide source originating from the middle of the Afternoon Creek slope, assuming worst case scenario parameters: (a) starting source volume depth and calculated deposit depth; and (b) calculated maximum velocities.



present-day slope would reach the SR-20 highway via the Afternoon Creek travel path during a rapid runout event. This loose debris might later present a hazard though in the form of potentially reactivating as a debris flow during a heavy-precipitation event, similar to those that have closed the SR-20 highway in the past. In a more direct sense, the runout models do show that any slope failures originating at or above the crest of the Afternoon Creek ridge have the potential to send a small volume of material down the Falls

**Fig. 20.** DAN3D forward analysis and runout assessment for a rockslide source originating from the top of the Afternoon Creek ridge, assuming worst case scenario parameters: (a) starting source volume depth and calculated deposit depth; and (b) calculated maximum velocities.



Creek travel path. Any rock that enters the Falls Creek travel path is likely to reach the SR-20 highway because the slope is steep and the travel path involves bare, hard bedrock with little vegetation. To contend with the rockfall hazard from Falls Creek, a protective embayment was constructed next to the highway in February 2006 (Fig. 21). A thorough study of rockfall trajectory and energy at the base of Falls Creek was completed to design the embayment. Based on the DAN3D results, in the event of a larger

**Fig. 21.** Protective embayment on Washington State Route 20 at Falls Creek completed in 2006. Photograph courtesy of Tom Badger (Washington State Department of Transportation).



rockslide initiating at the ridge and pushing material down Falls Creek, this material would impact the embayment with maximum velocities of up to 20–25 m/s. It should be noted that the function of the embayment is to protect from rockfalls and not from a large-volume rockslide, although partial protection would be provided because these types of barrier systems, constructed with soil, geofabric, and gabions, can absorb impact energies of up to 5000 kJ (Wyllie and Mah 2004).

## Conclusions

The rock-slope hazard investigation reported here presents a framework that links back analyses with forward modelling of rock-slope failure initiation and runout. These were used to assess the location, volume, and effects of a future rockslide at Afternoon Creek and Falls Creek above Washington State Route 20. A detailed field investigation, aided by terrestrial laser scanning, was used to collect discontinuity and rock mass characterization data together with topographic data of the ridge that serves as the source for the rocksliding activity. Structural geology and topographic controls were analyzed using a combination of kinematic analysis and 2D and 3D distinct-element modelling (UDEC and 3DEC). Rockslide runout was analyzed with the 3D dynamic analysis code, DAN3D.

The results from these analyses show that the 2003 Afternoon Creek rockslide originated along a ridge that divided and directed the 750 000 m<sup>3</sup> total volume down travel paths along both the front side (Afternoon Creek) and back side (Falls Creek) of the ridge. The primary failure mechanism was planar-sliding along a highly persistent joint set that dips approximately 50° and daylights into Afternoon Creek. A second steeply dipping but less persistent joint set provided rear release. No evidence was found of structurally controlled failure that displaced towards Falls Creek. The small percentage of material that travelled down Falls Creek entered the travel path due to the ridge topography.

Forward analyses using input and constraints provided by the back analyses indicate that the Afternoon Creek ridge still presents a danger and there is potential for a large rock-

slide event, albeit smaller in volume than the 2003 rockslide. Numerical models and field observations of the present-day slope conditions suggest that there are two potential source zones. The most threatening source zone is located at the crest above the 2003 rockslide back scarp. The failure mechanism here may be toppling of individual columns (approximate volume of 1 000 m<sup>3</sup> per column) or sliding towards Afternoon Creek (maximum volume of 100 000 m<sup>3</sup>). The DAN3D runout analysis indicates that both failure mechanisms have the potential to cause rock debris to enter the Falls Creek travel path and impact the recently constructed embayment adjacent to the highway. Rockslide or rockfall debris entering the Afternoon Creek travel path is unlikely to reach the highway.

The integrated methodology developed greatly facilitated the hazard assessment required for Afternoon Creek by providing a framework in which the results from each step of the analysis could be used to provide important mechanistic insights, constraints, and calibration input to subsequent parts of the analysis. Iterating between the different analytical tools used provided a means to overcome the limitations and uncertainties of each individual analysis and maximize our understanding of the complex rock mass and slope processes contributing to the hazard. The data-collection program was optimized for the numerical modelling work carried out, and hypotheses concerning the slope geometry and operative failure mechanisms could be tested and answer questions that were left unresolved by the other analyses.

## Acknowledgements

The authors would like to thank Tom Badger and the Washington State Department of Transportation, Dr. Robert L. Burk and URS Corp., and Norm Norrish and Wyllie & Norrish Rock Engineers for their assistance during the course of this investigation. Additional thanks are extended to Drs. Oldrich Hungr (The University of British Columbia) and Scott McDougall (BGC Engineering Inc.) for their assistance with the DAN3D modelling. This work was supported in part by an Natural Sciences and Engineering Research Council of Canada (NSERC) Discovery Grant and the Washington State Department of Transportation.

## References

- Barton, N. 1976. The shear strength of rock and rock joints. *International Journal of Rock Mechanics and Mining Sciences & Geomechanics Abstracts*, **13**(9): 255–279. doi:10.1016/0148-9062(76)90003-6.
- Eberhardt, E., Stead, D., and Coggan, J.S. 2004. Numerical analysis of initiation and progressive failure in natural rock slopes — the 1991 Randa rockslide. *International Journal of Rock Mechanics and Mining Sciences*, **41**(1): 69–87. doi:10.1016/S1365-1609(03)00076-5.
- Hart, R.D. 1993. An introduction to distinct element modeling for rock engineering. *In Comprehensive Rock Engineering: Principles, Practice & Projects*. Edited by J.A. Hudson. Pergamon Press, Oxford, UK. pp. 245–261.
- Hoek, E., and Brown, E.T. 1997. Practical estimates of rock mass strength. *International Journal of Rock Mechanics and Mining Sciences*, **34**(8): 1165–1186. doi:10.1016/S1365-1609(97)80069-X.



- Hoek, E., Carranza-Torres, C., and Corkum, B. 2002. Hoek–Brown Failure Criterion — 2002 Edition. *In Mining and Tunnelling Innovation and Opportunity: Proceedings of the 5th North American Rock Mechanics Symposium*, Toronto, 7–10 July 2002. Edited by R. Hammah, W. Bawden, J. Curran, and M. Telesnicki. University of Toronto, Toronto, Ont. Vol. 1, pp. 267–273.
- Hungr, O. 1995. A model for the runout analysis of rapid flow slides, debris flows, and avalanches. *Canadian Geotechnical Journal*, **32**(4): 610–623. doi:10.1139/t95-063.
- Hungr, O., and Evans, S.G. 1996. Rock avalanche run-out prediction using a dynamic model. *In Proceedings of the 7th International Symposium on Landslides*, Trondheim, Norway, 16–21 June 1996. Edited by K. Senneset. A.A. Balkema, Rotterdam, the Netherlands. Vol. 1, pp. 233–238.
- Itasca Consulting Group, Inc. 2003. 3DEC: User's guide, version 3.0. Itasca Consulting Group, Inc., Minneapolis, Minn.
- Itasca Consulting Group, Inc. 2004. UDEC: User's guide, version 4.0. Itasca Consulting Group, Inc., Minneapolis, Minn.
- Kulhawy, F.H. 1975. Stress deformation properties of rock and rock discontinuities. *Engineering Geology*, **9**(4): 327–350. doi:10.1016/0013-7952(75)90014-9.
- Marinos, P., and Hoek, E. 2000. GSI: a geologically friendly tool for rock mass strength estimation. *In Proceedings of GeoEng2000, An International Conference on Geotechnical and Geological Engineering*, Melbourne, Australia, 19–24 November 2000. Technomic Publishing Company Inc., Lancaster, Penn. pp. 1422–1440.
- McDougall, S., and Hungr, O. 2004. A model for the analysis of rapid landslide motion across three-dimensional terrain. *Canadian Geotechnical Journal*, **41**(6): 1084–1097. doi:10.1139/t04-052.
- McDougall, S., Pirulli, M., Hungr, O., and Scavia, C. 2008. Advances in landslide continuum dynamic modeling. *In Proceedings of the 10th International Symposium on Landslides and Engineered Slopes*, Xi'an, China, 30 June – 4 July 2008. Edited by Z. Chen, J.-M. Zhang, K. Ho, F.-Q. Wu, and Z.-K. Li. Taylor & Francis, London, UK. Vol. 1, pp. 145–157.
- Stead, D., Eberhardt, E., and Coggan, J.S. 2006. Developments in the characterization of complex rock slope deformation and failure using numerical modelling techniques. *Engineering Geology*, **83**(1–3): 217–235. doi:10.1016/j.enggeo.2005.06.033.
- Strouth, A. 2006. Integrated use of terrestrial laser scanning and advanced numerical methods for a total slope analysis of Afternoon Creek, Washington. M.Sc. thesis, Geological Engineering, University of British Columbia, Vancouver, B.C.
- Strouth, A., Burk, R.L., and Eberhardt, E. 2006. The Afternoon Creek Rockslide near Newhalem, Washington. *Landslides*, **3**(2): 175–179. doi:10.1007/s10346-005-0030-z.
- Wyllie, D.C., and Mah, C.W. 2004. *Rock slope engineering*. 4th ed. Spon Press, New York.